Automated Onboard Modeling of Cartridge Valve Flow Mapping

Song Liu and Bin Yao, *Member, IEEE*

***Abstract*—Proportional poppet-type cartridge valves are the key elements of the energy-saving programmable valves, which have been shown to be able to achieve good motion control performance while significantly saving energy usage in our previous studies. Unlike costly conventional four-way valves, the cartridge valve has a simple structure and is easy to manufacture, but the complicated mathematical model of its flow mapping makes the controller design and implementation rather difficult. Although off-line individually calibrated or manufacturer supplied flow mappings of the cartridge valves can be used, neither method is ideal for wide industrial applications. The former method is time-consuming and needs additional flow sensors while the latter may lead to significantly degraded control performance due to the inaccuracy of the manufacturer supplied flow mappings. Furthermore, due to inevitable system worn out and/or changing working conditions, actual cartridge valve flow mapping may change significantly over the life span of the system and need to be updated periodically in order to maintain the same level of control performance. Sometime, it may be even impractical to do off-line calibrations once the valve leaves the manufacturing plant. To solve this practically significant problem, this paper focuses on the automated onboard modeling of the cartridge valve flow mappings without using any extra sensors and removing the valves from the system. The estimation of flow mappings is based on the pressure dynamics of the hydraulic cylinder with the consideration of effects of some unknown system parameters such as the effective bulk modulus of the working fluid. Localized orthogonal basis functions are proposed to bypass the lack of persistent exciting identification data over the entire domain of the flow mapping during onboard experiments. Experimental results are obtained to illustrate the effectiveness and practicality of the proposed novel automated modeling method.**

***Index Terms*—Electrohydraulics, nonlinear system identification, onboard modeling, parameter estimation, valves.**

I. Introduction

THE energy-saving programmable valves, a combination of five independently controlled cartridge valves (Fig. 1), have been shown in our previous studies [1], [2] to successfully achieve the dual objectives of high-level motion control performance and significant energy saving. Such a capability comes from the decoupled meter-in and meter-out flows, the true cross port regeneration flow, and the increased flexibility and controllability of a multiple-input system. The key physical element of the programmable valves is the proportional poppet-type cartridge valve, which is a low accuracy but fast response valve widely used in industry due to its small size and low cost [3], [4].

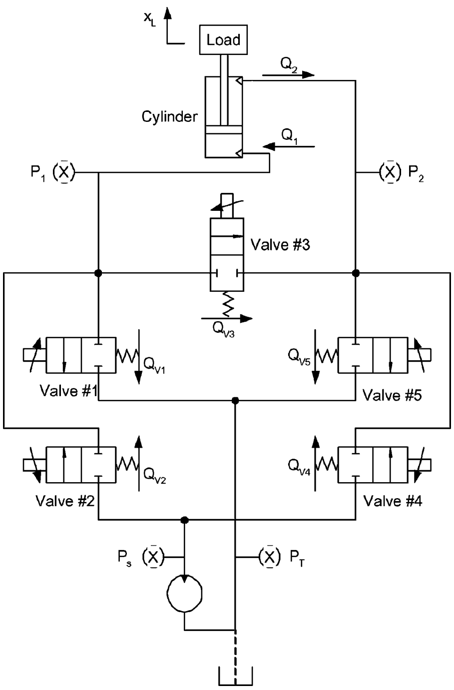

Fig. 1. Energy-saving programmable valves.

The programmable valves are designed and proposed as low-cost and energy-saving alternatives of expensive servo valves. They are used in precision motion control applications in hydraulic and manufacturing industry. The faster response of the poppet-type cartridge valves makes it more reasonable to neglect valve dynamics in the overall controller design process [5]; neglecting valve dynamics significantly simplifies the design of advanced nonlinear adaptive robust controllers [6] and has been a common practice in almost all recently developed advanced controls of electrohydraulic systems. With this simplification, the proportional cartridge valve can be modelled as a static nonlinear flow mapping from the input signal and the pressure drop across the valve into the flow rate through the valve. However, unlike the conventional four-way valves, the mathematical model of the cartridge valve flow mapping is much more complicated and cannot simply be described by some analytical nonlinear equations [7]–[10]. Cartridge valves have desirable physical properties (e.g., faster response) and the ability of bypassing the

Manuscript received October 31, 2005; revised April 22, 2006. Recommended by Guest Editors K. M. Lee and S. Chiaverini. This work was supported in part by the US National Science Foundation under Grant CMS-0220179 and in part by the National Natural Science Foundation of China (NSFC) under the Joint Research Fund 50528505 for Overseas Young Scholars. This paper was presented in part at the 2005 IEEE/ASME Conference on Advanced Intelligent Mechatronics (AIM'05).

S. Liu is with Hurco Companies, Inc., Indianapolis, IN 46268 USA.

B. Yao is with the School of Mechanical Engineering, Purdue University, West Lafayette, IN 47907 USA, and also with of the State Key Laboratory of Fluid Power Transmission and Control, Zhejiang University, Hangzhou 310027, China (e-mail: byao@purdue.edu).

Digital Object Identifier 10.1109/TMECH.2006.878552

sandwiched deadband control problem of the conventional four-way valves when connected as in the proposed programmable valves [5], but their uses have been traditionally limited to low-cost applications where precision motion control is not of major concern due to the practical problem of modeling them accurately with analytical nonlinear functions similar to those used in four-way valves. Our previous researches on the control of the programmable valves are based on either the individually calibrated valve flow mappings or the manufacturer supplied flow mapping. Using the individually calibrated flow mappings of the cartridge valves and a properly designed adaptive robust controller (ARC), it was shown in [2], [5] that a control performance similar to that using expensive servo valves can be achieved. However, in addition to the need of a flow calibration system that increases cost, individually calibrating each of the five cartridge valves is a very time-consuming task, which would prohibit the widespread use of the programmable valves in industry. Furthermore, the cartridge valve flow mapping may change significantly as the system ages and gets worn-out [11], and need to be updated regularly to maintain consistent control performance. For some applications, it may not even be possible to disassemble the valves from the systems for the time-consuming off-board calibrations. However, though the manufacturer supplied flow mapping can be used to design stable adaptive robust controllers as done in our previous study [12], the large modeling error of the manufacturer supplied flow mapping significantly limits the achievable control performance in practice. Thus, automated and yet accurate onboard modeling of cartridge valve flow mappings without taking the cartridge valves off the system becomes the key to the widespread use of programmable valves without having a compromised control performance, which is the focus of the paper and *serves as a practical example of the integrated mechatronics design philosophy of trading system hardware complexity with advanced software modeling and controls*.

To model the valve flow mappings, the input signal to the valve, the pressure drop across the valve, and the flow rate going through the valve need to be determined. The input signal and the pressure drops are usually known or measured. However, there are no sensors to measure the flow rate in an actual system. In [13], an attempt was made to build a flow rate observer based on the pressure dynamics of the controlled system via the sliding mode observer design technique. As the flow rate appears in the input channel and is not a state in the pressure dynamics, the resulting flow rate observers are subject to effects of certain unavoidable parametric uncertainties (e.g., the effective bulk modulus of hydraulic fluid) due to the changing working conditions. In this paper, a conceptually different approach will be taken into account. Namely, instead of determining the model parameters of the flow mapping based on the explicit flow rate measurement or estimation, the flow mapping model parameters and other unknown system parameters will be determined simultaneously from the pressure dynamics of the controlled system via certain intelligent integration of online parameter estimation algorithms and neural network type nonlinear function modeling techniques.

Another obstacle encountered in any onboard modeling attempt is due to the limited experiments that can be run on an actual machine. Unlike off-board modeling where deliberate tests can be performed to cover the entire working range of a valve, the loading conditions of any onboard experiment may be limited, making it impossible to obtain sufficient experimental data needed for an accurate estimation of all model parameters of a valve over its entire working envelope. To bypass this unique practical problem associated with the onboard modeling, localized orthogonal basis functions along with smooth blending and extrapolation are proposed in this paper. Experimental conditions for an accurate parameter estimations in a local region are carefully examined to obtain practical onboard tests that can be run for accurate modeling of all valve flow mappings in the active working regions of the overall system. Comparative experimental results are presented to illustrate the effectiveness and the achievable control performance of the proposed method in implementation.

II. Problem Formulation

Neglecting the valve dynamics, all valves can be modeled as a static function mapping the input signal and the pressure drop across the valve into the metered flow rate

$$Q(u, \Delta P) = C_d A_v(x_v(u, \Delta P))\sqrt{\frac{2}{\rho}}\sqrt{\Delta P} \tag{1}$$

where $Q(u, \Delta P)$ is the metered flow rate through the valve orifice, C_d is the discharge coefficient, $A_v(x_v)$ represents the orifice flow area, which is a function of the valve spool or poppet displacement x_v, and x_v depends on the input signal u and the pressure drop ΔP across the orifice, ρ is the fluid mass density.

For the conventional four-way valves such as the servo valves or the proportional directional control (PDC) valves, A_v is a linear function of x_v, which is only a linear function of input u and not affected by ΔP. Therefore the flow mapping model for four-way valves can be simplified to an analytical nonlinear function as

$$Q = k_q u\sqrt{\Delta P} \tag{2}$$

where k_q is the lumped valve parameter. As the above flow mapping involves at most one unknown parameter k_q, it is quite easy to obtain a reliable estimate of k_q through either off-line or online parameter estimation algorithm.

For cartridge valves, the flow forces and fluid inertance effects are in-line with the valve element and therefore play a much significant role than that in a spool valve. The relationship between A_v and x_v is therefore highly nonlinear and depends on the specific valve construction structure. Cartridge valves from different manufactures may have different nonlinear functions to connect x_v and A_v. It may also change noticeably as the system starts wears out. Furthermore, the pressure drop ΔP affects the valve opening significantly, and thus the resulting flow mapping cannot be simply expressed by analytical nonlinear functions like (2). In fact, the function $x_v(u, \Delta P)$ is very complicated and highly nonlinear, and usually contains some deadband regions and hard limits [2], [5], [11]. One has to treat the cartridge valve flow mapping as an unknown nonlinear function $Q(u, \Delta P)$ and seek another approach to deal with this problem.

There are many ways to approximate an unknown function, such as the neural network [14], Fourier decomposition [15], Wavelet decomposition [16], and so on. The basic idea of all the approximation methods is to decompose an unknown function into a set of basis functions with certain weighting factors. With this concept, the nonlinear flow mapping function can be decomposed as

$$Q(u, \Delta P) = \bar{Q}(u, \Delta P) + \Delta, \quad \bar{Q} = \varphi^T(u, \Delta P) w \tag{3}$$

where $\varphi^T = [\varphi_1, \varphi_2, \ldots, \varphi_n]$ is a finite dimension vector of basis functions, and $w^T = [w_1, w_2, \ldots, w_n]$ is a vector of unknown parameters or weighting factors, and Δ represents the approximation error. However, straightforward application of the above neural network approximation seldom leads to satisfactory flow mapping model due to the following practical limitation. In order to have a reasonably small approximation error Δ, a large number of neurons (i.e., large n) have to be used. This is especially true for the cartridge valve flow mapping due to the nonsmoothness of the cartridge flows caused by the discontinuous frictions of the valve and the difficulty of traditional neural networks in approximating nonsmooth functions. Consequently, to obtain the flow mapping model $\bar{Q}(u, \Delta P)$, a large number of parameters $\theta = w$ have to be adapted or estimated simultaneously from the limited experimental data sets. This makes it difficult to use the well-known parameter estimation algorithms having better converging properties due to the difficulty of running onboard experiments to satisfy the experimental conditions needed by these algorithms. For example, the least square estimation (LSE) algorithm needs the persistent excitation condition for convergence of parameter estimates, which, loosely speaking, can be satisfied only if rich enough data sets covering the entire working envelope of the control input u and the pressure drop ΔP are available. However, for onboard flow modeling where the valves cannot be removed from the actual system, ΔP depends on the loading conditions of the overall system and is not an experimental variable that can be freely controlled. As a result, there may be no way to conduct experiments that cover the entire range of ΔP. To bypass this problem, localized basis functions will be used as detailed in Section III.

As the actual valve flow rates cannot be measured, they have to be estimated based on other available onboard measurements as follows. Neglecting cylinder leakages, the cylinder pressure dynamics can be written as [17]

$$\begin{aligned} \frac{V_1(x_L)}{\beta_e}\dot{P}_1 &= -A_1\dot{x}_L + Q_1(u_1, \Delta P_1) \\ \frac{V_2(x_L)}{\beta_e}\dot{P}_2 &= +A_2\dot{x}_L - Q_2(u_2, \Delta P_2) \end{aligned} \tag{4}$$

where $V_1(x_L)$ and $V_2(x_L)$ are the total cylinder volumes of the head-end and rod-end sides including connecting hose volumes respectively, x_L is the displacement of the cylinder rod, β_e is the effective bulk modulus, P_1 and P_2 represent the pressures in the head-end and rod-end sides, respectively, A_1 and A_2 are the head-end and rod-end ram areas of the cylinder, Q_1 and Q_2 are the supply and return flow rates, respectively, u_1 and u_2 are the input signals to the valves, and ΔP_1 and ΔP_2 are the pressure drops across the valves. In (4), A_1 and A_2 are known parameters, u_1 and u_2 are control signals sent out by the controller, x_L, P_1, P_2, ΔP_1, and ΔP_2 are measurable, and $V_1(x_L)$ and $V_2(x_L)$ are calculable. The effective bulk modulus β_e is usually an unknown parameter and changes significantly with working conditions and components such as tubes, cylinder design, and hoses. As the pressure dynamics in the rod-end side has the same form as the one in the head-end side, in the following discussion, only the head-end pressure dynamics is used to demonstrate the method of solving the problem.

Defining $\theta_{\beta_e} = 1/\beta_e$, and assuming that the nonlinear flow rate $Q_1(u_1, \Delta P_1)$ is decomposed into the form given by (3), the head-end pressure dynamics can then be rewritten as

$$A_1\dot{x}_L = -V_1(x_L)\dot{P}_1\theta_{\beta_e} + \varphi(u_1, \Delta P_1)^T\theta + \Delta. \tag{5}$$

Defining $\varphi_{\text{new}}^T = [-V_1(x)\dot{P}_1 \quad \varphi(u_1, \Delta P_1)^T]$ and $\theta_{\text{new}}^T = [\theta_{\beta_e} \quad \theta^T]$, (5) can be written in a compact form as

$$A_1\dot{x} = \varphi_{\text{new}}^T \cdot \theta_{\text{new}} + \Delta. \tag{6}$$

Equation (6) is in the standard linear regression form with respect to the unknown parameter θ_{new} with $A_1\dot{x}$ being the model output and Δ the model error; both the model output and the regressor can be calculated based on the onboard sensor measurements. Thus, the original problem of automated onboard flow mapping modeling in the presence of unknown system parameters is transformed into the tractable problem of accurate parameter estimation based on the linear regression model (6). The rest of the paper thus focuses on the selection of suitable basis functions $\varphi(u_1, \Delta P_1)$, the design of experiments, and the use of the LSE to minimize the effect of model error Δ for accurate parameter estimation.

III. Localized Basis Functions and Smooth Blending for Approximation of Two-Dimensional Functions

To better explain the underlying working principles of the proposed method, for time being, it is assumed in this section that the valve flow rate $Q(u, \Delta P)$ is available for the flow mapping modeling, i.e., assuming that certain onboard experiments that cover all possible actual working conditions have been performed with the inputs and the measured valve pressure drops and the valve flow rate given by $\{u(t), \Delta P(t), Q(t), t = 1, 2, \ldots, N\}$ respectively, where N represents the total number of sample data from all experiments. In this case, if the neural network type flow mapping model given by (3) is used, then

$$[Q] = \Phi\theta + [\Delta] \tag{7}$$

where $[Q] = [Q(1), Q(2), \ldots, Q(N)]^T$ is the vector of flow rate measurements, $\Phi = [\varphi(u(1), \Delta P(1)),\ \varphi(u(2), \Delta P(2)), \ldots, \varphi(u(N), \Delta P(N))]^T$ can be calculated based on the input and the measured valve pressure drops, and $[\Delta] = [\Delta(1), \Delta(2), \ldots, \Delta(N)]^T$ is the vector of neural network approximation errors which are bounded but unknown. If Φ has full-column rank, then the optimal estimation of θ in the sense of the LSE error is given by

$$\hat{\theta} = \Phi^+[Q] \tag{8}$$

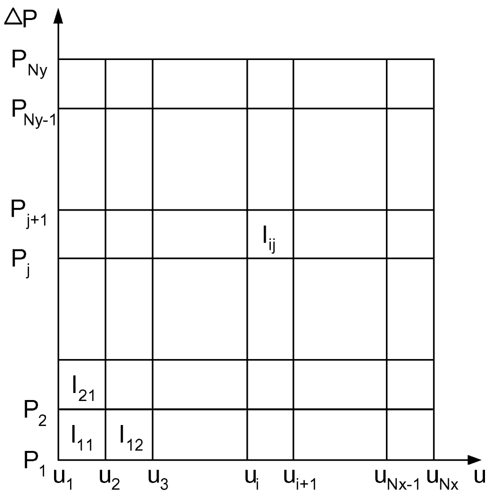

Fig. 2. Cutting the $u - \Delta P$ surface into small blocks.

where $\Phi^+ = (\Phi^T \Phi)^{-1}\Phi^T$ is the pseudo inverse of Φ. Substituting (7) into (8), the LSE parameter estimation error $\tilde{\theta} = \hat{\theta} - \theta$ is given by

$$\tilde{\theta} = \Phi^+[\Delta] = (\Phi^T \Phi)^{-1}\Phi^T[\Delta] \tag{9}$$

As discussed in the problem formulation, with the above traditional neural network model, to have a reasonable small model approximation error $[\Delta]$, the dimension of the basis function n has to be very high, especially when the unknown function to be approximated has discontinuity or nondifferentiable points. This fact plus the additional practical limitation of not being able to run onboard experiments to excite the system for a variety of pressure drops makes it impossible to satisfy the condition needed to apply the above LSE algorithm—Φ being full column rank, or equivalently, $\Phi^T\Phi$ being invertible. To solve this problem, in the following discussion, localized basis functions with smooth blending will be used.

Due to the fact that the cartridge valve can only accept bounded input signal u ranging from 0 to 10 V and the pressure drop is also limited, the flow mapping is defined only on a compact support. It is reasonable to cut the support on $u - \Delta P$ surface into small blocks. Each block is named after the indices of u and P, e.g., I_{ij}, as shown in Fig. 2, where u_{Nx} and P_{Ny} represent the maximal values of u and ΔP, respectively. The distances between u_i and u_{i+1} or P_i and P_{j+1} do not have to be equally spaced. As the function approximation will be done on each small block instead of on the entire region, *a priori* knowledge about the flow mapping can be used to choose the spacing to have a reasonable good model approximation accuracy while minimizing the number of blocks needed. For example, it is known that the deadband may happen around some input values though the exact value is not known. Thus, relatively small spacing should be used in regions near those input values. However, at the regions where one knows the flow mapping may not change drastically, relatively larger spacings can be used to reduce the computation load.

On each small block I_{ij}, the valve flow rate does not change drastically and may be approximated by a Taylor series with respect to the nominal point

$$\begin{aligned} Q(u, \Delta P)|_{(u,\Delta P)\in I_{ij}} &= Q(\bar{u}_i, \Delta\bar{P}_j) + \left.\frac{\partial Q}{\partial u}\right|_{(\bar{u}_i, \Delta\bar{P}_j)} \tilde{u} + \left.\frac{\partial Q}{\partial \Delta P}\right|_{(\bar{u}_i, \Delta\bar{P}_j)} \tilde{P} \\ &\quad + \frac{1}{2}\left.\frac{\partial^2 Q}{\partial u^2}\right|_{(\bar{u}_i, \Delta\bar{P}_j)} \tilde{u}^2 + \frac{1}{2}\left.\frac{\partial^2 Q}{\partial \Delta P^2}\right|_{(\bar{u}_i, \Delta\bar{P}_j)} \tilde{P}^2 \\ &\quad + \frac{1}{2}\left.\frac{\partial^2 Q}{\partial u \partial \Delta P}\right|_{(\bar{u}_i, \Delta\bar{P}_j)} \tilde{u}\tilde{P} + \Delta \end{aligned} \tag{10}$$

where $(\bar{u}_i, \Delta\bar{P}_j)$ represents the nominal working point in the block of I_{ij}, $\tilde{u} = u - \bar{u}_i$ and $\tilde{P} = \Delta P - \Delta\bar{P}_j$, and Δ represents the lumped effect of all higher order terms and modeling error. *A priori* knowledge about the flow mapping as well as the required model approximation accuracy can be used to determine how many terms to keep. For simplicity, in this paper, all terms up to second order are kept while all higher order terms are considered as modeling error. The valve flow rate in the block of I_{ij} is thus approximated by a model given by

$$\bar{Q}(u, \Delta P)|_{(u,\Delta P)\in I_{ij}} = \varphi_{ij}^T \theta_{ij} \tag{11}$$

where

$$\varphi_{ij}^T = \begin{cases} [1, \quad \tilde{u}, \quad \tilde{P}, \quad \tilde{u}^2, \quad \tilde{P}^2, \quad \tilde{u}\tilde{P}], & (u, \Delta P) \in I_{ij} \\ [0, \quad 0, \quad 0, \quad 0, \quad 0, \quad 0], & \text{otherwise} \end{cases}$$

and

$$\begin{aligned} \theta_{ij} = \Bigg[& Q(\bar{u}_i, \Delta\bar{P}_j), \quad \left.\frac{\partial Q}{\partial u}\right|_{(\bar{u}_i, \Delta\bar{P}_j)}, \left.\frac{\partial Q}{\partial \Delta P}\right|_{(\bar{u}_i, \Delta\bar{P}_j)} \\ & \left.\frac{\partial^2 Q}{\partial u^2}\right|_{(\bar{u}_i, \Delta\bar{P}_j)}, \left.\frac{\partial^2 Q}{\partial \Delta P^2}\right|_{(\bar{u}_i, \Delta\bar{P}_j)} \\ & \left.\frac{\partial^2 Q}{\partial u \partial \Delta P}\right|_{(\bar{u}_i, \Delta\bar{P}_j)} \Bigg]^T \in \mathbb{R}^6. \end{aligned}$$

As $\varphi_{ij} = 0$ when its arguments $\tilde{u}$ and $\tilde{P}$ are outside the block I_{ij}, $\varphi_{ij}^T \varphi_{kl} = 0$ if either $i \neq k$ or $j \neq l$. Thus, the basis functions φ_{ij} are orthogonal.

With the above local approximations, the approximated flow mapping model for the entire region is

$$\bar{Q}(u, \Delta P) = \sum_{j=1}^{N_y} \sum_{i=1}^{N_x} \varphi_{ij}^T \theta_{ij}. \tag{12}$$

Equation (12) is in the form of (3) with

$$\varphi^T = [\varphi_{11}^T, \varphi_{12}^T, \ldots, \varphi_{1N_y}^T, \varphi_{21}^T, \ldots, \varphi_{ij}^T, \ldots, \varphi_{N_x N_y}^T]$$

and

$$\theta^T = [\theta_{11}^T, \theta_{12}^T, \ldots, \theta_{1N_y}^T, \theta_{21}^T, \ldots, \theta_{ij}^T, \ldots, \theta_{N_x N_y}^T].$$

However, unlike (3), the basis functions φ_{ij} in (12) are localized, which enables accurate parameter estimations to be carried out for individual blocks where sufficient data exist and the condition for applying the LSE algorithm is satisfied. These regions normally correspond to the actual active working ranges that the system is likely to operate, and thus precise flow modeling in these regions is important for good control performance. The details are given below.

Regroup the sample data according to the blocks they belong to. For simplicity, assume that $\{u(t), \Delta P(t), Q(t), t = 1, 2, \ldots, N_{ij}\}$ are the set of sample data falling into the block I_{ij}, i.e., $(u(t), \Delta P(t)) \in I_{ij}, \forall t = 1, 2, \ldots, N_{ij}$ where N_{ij} represents the number of points. From (10) and (11), a similar form as (7) can be obtained for the block I_{ij}

$$[Q(u, \Delta P)]|_{(u,\Delta P)\in I_{ij}} = \Phi_{ij}\theta_{ij} + [\Delta] \tag{13}$$

where $[Q(u, \Delta P)]|_{(u,\Delta P)\in I_{ij}}$ represents the vector of the measured valve flow rate and $\Phi_{ij} = [\varphi_{ij}(1), \varphi_{ij}(2), \ldots, \varphi_{ij}(N_{ij})]^T$. If $\Phi_{ij}^T\Phi_{ij}$ is invertible—a condition that can be satisfied relatively easily due to the small number of parameters to be estimated, then, the experimental data are sufficient to give a good LSE estimate of θ_{ij} on the block I_{ij}

$$\hat{\theta}_{ij} = \left(\Phi_{ij}^T\Phi_{ij}\right)^{-1}\Phi_{ij}^T[Q(u, \Delta P)]|_{(u,\Delta P)\in I_{ij}}. \tag{14}$$

In practice, one can check the condition number of $\Phi_{ij}^T\Phi_{ij}$ instead of its invertibility to make sure that the above estimation is numerically well-conditioned for reliable estimations.

For the blocks where $\Phi_{ij}^T\Phi_{ij}$ is not invertible or ill-conditioned, it is impossible to have an accurate estimate of θ_{ij} as the experimental data obtained do not provide enough information on I_{ij} for flow modeling. Therefore one should not force the system to estimate θ_{ij}. The flow mapping in these regions should be obtained via other means such as the extrapolation based on the flow models obtained for the blocks where accurate and sufficient data are available. The aim of the paper is to obtain a suitable model for control design. If a well-designed system ID experiment cannot excite the system in some regions, we do not expect the system would normally operate in those regions too. Therefore, the accuracy of the model in those regions is insignificant for control purpose, and it is not the focus of the paper to have an accurate model in those regions. The important issue that the paper cares about is to make sure that the lack of rich data sets in those poorly excited regions does not affect the system ID accuracy of the other regions. This is guaranteed by the localized estimation technique presented, which is the novel idea and key contribution of the paper.

The idea in the above-mentioned method is to pass a signal through a discontinuous rectangular window defined on each block I_{ij} that would result in discontinuous estimation of the discontinuities that happen at the block boundaries. To avoid these discontinuity artifacts, it is necessary to use smooth windows [16]. The lapped projectors, which split signal in orthogonal components with overlapping supports [16], are used to smooth the discontinuous estimation.

For simplicity, two orthogonal projectors that decompose any $f \in L^2(\mathbb{R})$ in two orthogonal components P^+f and P^-f whose supports are $[-1, +\infty)$ and $(-\infty, 1]$, respectively are constructed for demonstration, as illustrated in Fig. 3.

$$\begin{aligned} P^+f(t) &= \beta(t)[\beta(t)f(t) + \beta(-t)f(-t)] \\ P^-f(t) &= \beta(-t)[\beta(-t)f(t) - \beta(t)f(-t)] \end{aligned} \tag{15}$$

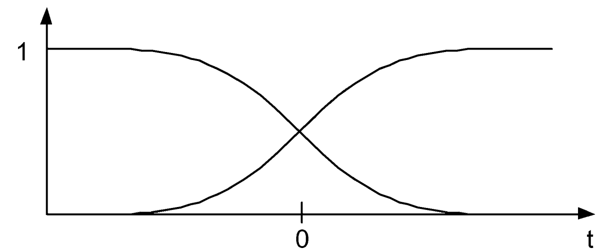

Fig. 3. Lapped orthogonal projectors.

where β is a monotonously increasing profile function having the properties that

$$\beta(t) = \begin{cases} 0 & \text{if } t < -1 \\ 1 & \text{if } t > 1 \end{cases}$$

and $\beta^2(t) + \beta^2(-t) = 1 \; \forall t \in [-1, 1]$.

1) Theorem 1: (Coifman and Meyer): The operators P^+ and P^- are orthogonal projectors, respectively, on W^+ and W^-. The spaces W^+ and W^- are orthogonal and $P^+ + P^- = \text{Identity}$.

The proof of the theorem can be referred to in [16]. The projectors can be easily shifted to $[a - \eta, +\infty)$ and $(-\infty, a + \eta]$ or repeated at different locations to perform a signal decomposition into orthogonal pieces whose supports overlap. It is also straight-forward to extend the projectors from one-dimensional (1-D) to two-dimensional (2-D). There exist several well-known lapped orthogonal bases, such as the family of local cosine functions [16].

In the above development, predetermined or fixed blocks are used for local parameter estimations. In general, at the expense of increased complexity, these blocks do not have to be fixed and real-time measurement data can be used to online cut the working range for a better local function approximation and parameter estimation, which is a topic of future research. For specific applications, like the identification of cartridge valve flow mapping detailed in the next section, enough *a priori* information exists to predetermine the necessary blocking. The use of fixed blocks may be more desirable due to its simplicity.

IV. Automated Onboard Modeling of Valve Flow Mappings

As discussed in the problem formulation, the actual valve flow rate is not measured in onboard experiments. However, with φ_{new} and θ_{new} in (6) defined as

$$\varphi_{\text{new}}^T = [-V_1(x)\dot{P}_1, \varphi_{11}^T, \varphi_{12}^T, \ldots, \varphi_{1N_y}^T, \varphi_{21}^T, \ldots, \varphi_{ij}^T, \ldots, \varphi_{N_xN_y}^T]$$

and

$$\theta_{\text{new}}^T = [\theta_{\beta_e}, \theta_{11}^T, \theta_{12}^T, \ldots, \theta_{1N_y}^T, \theta_{21}^T, \ldots, \theta_{ij}^T, \ldots, \theta_{N_xN_y}^T]$$

the same estimation technique as in the previous section can be used to obtain the estimates of θ_{β_e} and θ_{ij} simultaneously for the blocks where the local persistent excitation condition is satisfied.

In practice, although x_L, $\dot{x}_L$, ΔP_1, and $V_1(x_L)$ are measurable or calculable, $\dot{P}_1$ is neither measurable nor calculable by

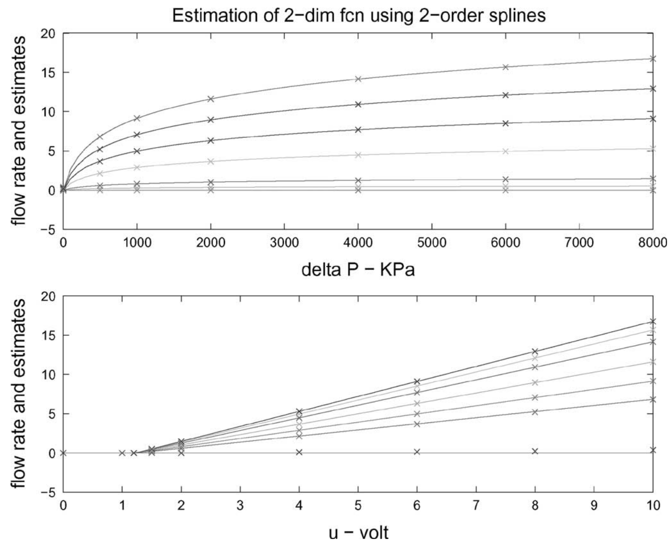

Fig. 4. Estimation of a 2-D function.

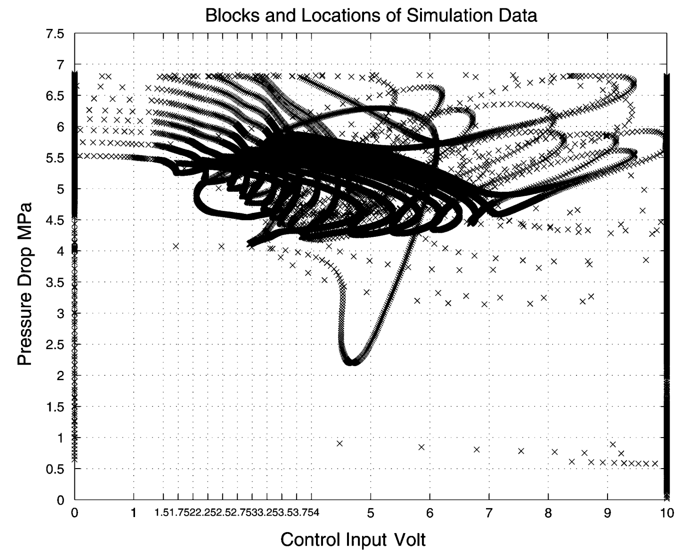

Fig. 5. Blocking and location of the experimental data.

differentiating P_1 due to the very noisy pressure measurement. The well-known low-pass filtering technique in adaptive control can be applied here to solve the problem [18]. Specifically, in order to make (6) implementable for parameter estimation algorithms, a low-pass filter, such as the one in (16), can be applied to the regressor $\varphi_{\rm new}$ as well as the virtual output $A_1\dot{x}$

$$H_f(s) = \frac{\omega_{\rm n}^2}{s^2 + 2\zeta\omega_{\rm n}s + \omega_{\rm n}^2} \tag{16}$$

where ζ and $\omega_{\rm n}$ are the damping ratio and natural frequency of the low-pass filter, respectively. Applying the linear filter (16) to both sides of (6) leads to

$$A_1\dot{x}_{Lf} = \varphi_{\rm newf}^T\theta_{\rm new} + \Delta_f \tag{17}$$

where $\dot{x}_{Lf}$, $\varphi_{\rm newf}^T$, and Δ_f represent the filtered $\dot{x}_L$, $\varphi_{\rm new}$, and Δ. With (17), the effect of measurement noise is reduced and the same estimation technique as in the previous section can still be used to obtain the estimates of θ_{β_e} and θ_{ij} simultaneously for the blocks where the local persistent excitation condition is satisfied.

V. Simulations and Experiments

Simulations and experiments were done to illustrate the effectiveness of the proposed automated onboard modeling technique for input nonlinearities. In the simulation, a nonsmooth 2-D nonlinear function was identified by the proposed method. Fig. 4 shows the simulation results, where the continuous curves represent the true value of the function while the X's represent the estimated values. As *a priori* knowledge may provide information about where the deadband would occur, e.g., between $u = 1$ and $u = 2$ in this simulation, relatively small spacing was chosen in this region. And relatively large spacing was set where the function does not change drastically.

In the experiments, the programmable valves were used to control the boom motion of a three-degree-of-freedom electro-hydraulic robot arm in the Ray W. Herrick Laboratories. The working mode selection and energy-saving controller design can be found in [2]. The boom motion was controlled to track a swiped sinusoidal reference trajectory, whose frequency varied from 0.1 to 0.5 Hz over 80 s. Fig. 5 shows how the blocks were generated and where the experimental data were located. The fine grids between 1 and 4 V for the control input were for more accurate flow estimation to deal with the unknown deadband in this region.

It was obvious that the obtained onboard experiment data did not cover the entire region, and it was impossible to have flow estimates in the blocks which suffered low data or no data at all. However, with the localized orthogonal basis functions and by checking the condition number of $\Phi_{ij}^T\Phi_{ij}$ on each block, one could easily control the estimation process with the proposed method. For example, by setting the threshold for the condition number as 1×10^8 and only estimating the flow mappings for blocks having the condition number less than the threshold, the estimated flow mapping was compared with the individually calibrated one as shown in Table I. In this table, the flow rate has a unit of liters/minute, the upper row of numbers represent the estimated flow mapping (the label "N A" indicates the block where the conditional number is larger than the set threshold) and the lower row of numbers were individually calibrated flow mapping. It is seen that both values were quite close to each other for the blocks where the condition numbers satisfy the set threshold, illustrating the reasonable modeling accuracy of the proposed method over the active working range of the system.

TABLE I
Estimated Flow Mapping Versus Calibrated One

	4v	5v	6v	7v
4.5MPa	7.33 8.00	12.02 11.83	17.79 17.57	22.96 22.60
5MPa	8.20 8.00	12.44 12.22	17.37 17.18	22.62 21.95
5.5MPa	7.98 7.97	12.02 12.00	NA 16.39	NA 20.61

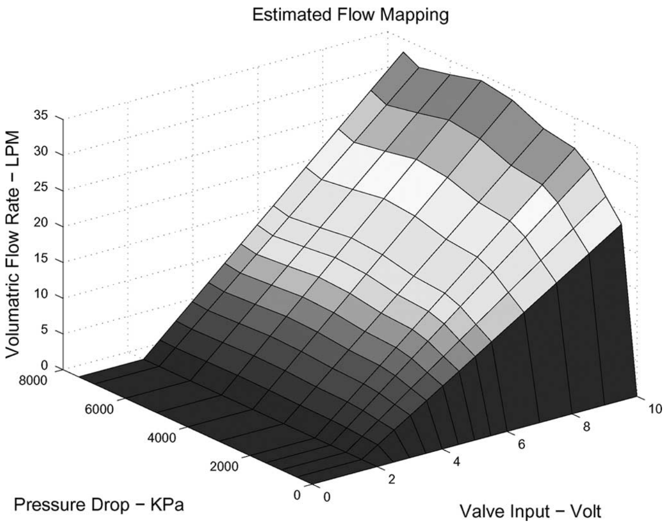

Fig. 6. Estimated cartridge valve flow mapping.

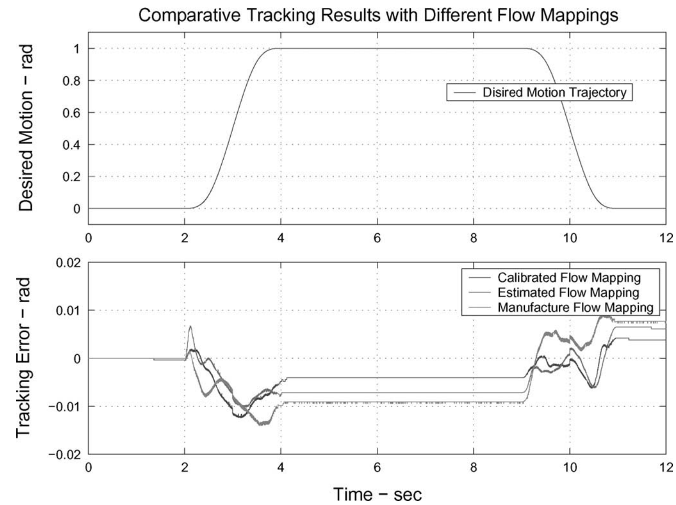

Fig. 7. Comparative tracking results with different flow mappings.

In the above study, neither the valve control input u nor the pressure drop ΔP was arbitrarily controlled. This resulted in lack of data in quite a large number of regions. For more accurate flow mapping estimation, one can simplify the 2-D flow mapping into a series of 1-D mappings, i.e., fix the control input u and estimate the 1-D function described as follows:

$$Q(u, \Delta P)|_{u=u_i} = Q_i(\Delta P), \quad i = 1, 2, \ldots, Nx. \tag{18}$$

Fig. 6 shows one of the experimentally estimated flow mappings with this simplified 1-D method.

To illustrate the effectiveness of the proposed method and check the accuracy of the estimated flow mapping, the above estimated flow mappings (a series of 1-D mapping) along with the individually calibrated one [2], [5] or the manufacturer supplied one [12] were used in the same ARC to control the boom motion of the hydraulic arm respectively. The ARC has an online adaptation loop to reduce the effect of modeling error and improve the tracking performance, especially steady-state error. The adaptation for the modeling error in the experiment was shut off for a better reflection of model inaccuracy. The control task was a smooth point-to-point motion trajectory as shown in Fig. 7. The trajectory included high acceleration and high speed tracking periods as well as constant positioning regulation periods, and reflected both of the two typical control problems—tracking control and positioning control. It was a very good evaluation to check the accuracy of the identified model. The tracking performances are shown in the second plot of Fig. 7. Although the controller with the experimentally estimated flow mappings performed not as good as the one with individually calibrated flow mappings, it did perform better than the one using the manufacturer supplied flow mappings.

One of the most important applications of the automated modeling technique is to update the valve flow mapping to address the issues of system aging and worn-out and change of working conditions or parameters. Due to the limitation of experimental setup, it is difficult to run experiments to show how well the proposed technique performs with a worn-out system or different working conditions. However, as the proposed technique is independent of system conditions, it is expected to achieve similar control performance after an update of flow mappings.

VI. Conclusion

Automated onboard modeling of the proportional cartridge valve flow mapping provides a simple and yet effective solution to obtain a suitable valve model for control design and to update the valve flow mapping to address the issues of system aging, worn out and changing parameters or working conditions after the system leaves the manufacturing plant. It is of significant importance for widespread industrial use of the valve in applications involving both precision motion control and energy saving. Due to the rather complicated and uncertain model structure of the cartridge valves, it was impossible to formulate the modeling of their flow mappings into some simple parameter estimation problems, not to mention the unavailability of the flow rate measurement and the uncertain parameters in the system dynamics. This paper proposed an approach to decompose and approximate the unknown flow mapping with some localized orthogonal basis functions. The weighting parameters of the basis functions as well as the unknown system parameters were then estimated simultaneously based on the pressure dynamics of the cylinder for regions where sufficient onboard measurement data were available. Smooth blending and extrapolation are subsequently applied to obtain the onboard estimation of the flow mapping over the entire working envelope of the system. Experimental studies have been obtained to demonstrate the feasibility of the proposed method for the automated onboard modeling of the cartridge valve flow mappings and the improvement of control performance with the estimated flow mappings. The paper thus serves well as a practical example of the integrated mechatronics design philosophy of trading system hardware complexity with advanced software modeling and controls. The strategy is general in principle and may be used in other systems with unknown static input nonlinearities of one or two dimensions.

REFERENCES

[1] S. Liu and B. Yao, "Energy-saving control of single-rod hydraulic cylinders with programmable valves and improved working mode selection," *SAE Trans.—J. Commercial Veh.*, pp. 51–61, 2002.
[2] ——, "Coordinate control of energy-saving programmable valves," in *Proc. ASME Int. Mech. Eng. Congr. Expo.*, Washington, DC, 2003, IMECE 2003-42668.
[3] J. J. Pippenger, *Hydraulic Cartridge Valve Technology.* Berlin: Amalgan, 1990.
[4] T. J. Ulery, "Propotional cartridge valves—economical alternative to large valves," *Agricultural Eng.*, vol. 71, no. 4, p. 11, 1990.
[5] S. Liu and B. Yao, "Programmable valves: a solution to bypass deadband problem of electro-hydraulic systems," in *Proc. Am. Control Conf.*, Boston, MA, 2004, pp. 4438–4443.
[6] B. Yao, F. Bu, J. T. Reedy, and G. T. Chiu, "Adaptive robust control of single-rod hydraulic actuators: theory and experiments," *IEEE/ASME Trans. Mechatron.*, vol. 5, no. 1, pp. 79–91, 2000.
[7] N. Vaughan and J. Gamble, "The modeling and simulation of a proportional solenoid valve," *ASME J. Dynam. Syst., Meas., Control*, vol. 118, pp. 120–125, 1996.
[8] N. Vaughan, D. Johnston, and K. Edge, "Numerical simulation of fluid flow in poppet valves," in *Proc. Inst. Mech. Eng.*, 1992, vol. 206, pp. 119–127.
[9] D. Johnston, K. Edge, and N. Vaughan, "Experimental investigation of flow and force characteristics of hydraulic poppet and disc valves," in *Proc. Inst. Mech. Eng.*, 1991, vol. 205, pp. 161–171.
[10] S. Liu, G. Krutz, and B. Yao, "Easy5 model of two position solenoid operated cartridge valves," in *Proc. ASME Int. Mech. Eng. Congree Expo.*, New Orleans, LA, 2002, IMECE 2002-39335.
[11] E. C. Fitch and I. T. Hong, *Hydraulic Component Design and Selection*. Stillwater, OK: BarDyne, Inc., 2001.
[12] S. Liu and B. Yao, "Adaptive robust control of programmable valves with manufacture supplied flow mapping only," presented at the IEEE Conf. Decision Control, Atlantis, Paradise Island, Bahamas, 2004.
[13] ——, "Sliding mode flow rate observer design," presented at the 6th Conf. Fluid Power Transmission Control, Hangzhou, China, 2005.
[14] S. Haykin, *Neural Networks, A Comprehensive Foundation,* 2nd ed. Delhi, India: Pearson Education, 1999.
[15] A. V. Oppenheim and R. W. Schafer, *Digital Signal Processing*. Englewood Cliffs, NJ: Prentice Hall, 1985.
[16] S. Mallat, *A Wavelet Tour of Signal Processing*. New York: Academic, 1999.
[17] H. E. Merritt, *Hydraulic Control Systems*. New York: Wiley, 1967.
[18] K. J. Åström and B. Wittenmark, *Adaptive Control*, 2nd ed. Reading, MA: Addison-Wesley, 1995.

Song Liu received the Ph.D. degree from the School of Mechanical Engineering, Purdue University, IN, in 2005.

He is currently a Principal Engineer at Hurco Companies, Inc., Indianapolis, IN, USA. His research interests include advanced control theory and applications, mechatronics, multiaxis coordinated precision motion control, fluid power system control, active noise and vibration control, and dynamic stream database control.

Bin Yao (M'91) received the Ph.D. degree in mechanical engineering from the University of California, Berkeley, in 1996, the M.Eng. degree in electrical engineering from the Nanyang Technological University, Singapore, in 1992, and the B.Eng. degree in applied mechanics from the Beijing University of Aeronautics and Astronautics, China, in 1987.

Since 1996, he has been with the School of Mechanical Engineering, Purdue University, IN, and was promoted to Associate Professor in 2002. He is one of the Kuang-piu Lecture Professors at Zhejiang University, Hangzhou, China and one of the Guest Professors at Shenzhen Graduate School of Harbin Institute of Technology, Shenzhen, China as well. His research interests include the design and control of intelligent high performance coordinated control of electro-mechanical/hydraulic systems, optimal adaptive and robust control, nonlinear observer design and neural networks for virtual sensing, modeling, fault detection, diagnostics, and adaptive fault-tolerant control, and data fusion.

Dr. Yao is the recipient of the O. Hugo Schuck Best Paper (Theory) Award from the American Automatic Control Council in 2004. He has been actively involved in various technical professional societies such as ASME and IEEE, He has been a member of the International Program Committee of a number of IEEE, ASME, and IFAC conferences. From 2000 to 2002, he was the Chair of the Adaptive and Optimal Control panel, and the Chair of the Fluid Control panel of the ASME Dynamic Systems and Control Division (DSCD) from 2001 to 2003. He currently serves as the Vice-Chair of the Mechatronics Technical Committee of ASME DSCD that he initiated in 2005. He has been a Technical Editor of the IEEE/ASME TRANSACTIONS ON MECHATRONICS since 2001. He was awarded a Faculty Early Career Development (CAREER) Award from the National Science Foundation (NSF) in 1998 for his work on the engineering synthesis of high performance adaptive robust controllers for mechanical systems and manufacturing processes, and a Joint Research Fund for Overseas Young Scholars from the National Natural Science Foundation of China (NSFC) in 2005.